Biophysical Chemistry, 34 (1989) 269–282
Elsevier

BIOCHE 01394

Application of method of moments analysis to fluorescence decay lifetime distributions

Louis J. Libertini and Enoch W. Small

Department of Biochemistry and Biophysics, Oregon State University, Corvallis, OR 97331, U.S.A.

Received 25 May 1989
Revised manuscript received 11 August 1989
Accepted 11 August 1989

Fluorescence decay; Decay-lifetime distribution; Method of moments analysis

In fluorescence decay work, distributions of exponential decay lifetimes are anticipated where complex systems are examined. We describe here methods of gaining information on such distributions using the method of moments analysis approach. The information obtained may be as simple as the average and deviation of the lifetime distribution, quantities which we show may be estimated directly from the results of a multiexponential analysis. An approximation to the actual distribution shape may also be obtained using a procedure we call the variable filter analysis (VFA) method without making any assumptions about the shape of the distribution. Tests of VFA using both simulated and experimental data are described. Limitations of this method and of distribution analysis methods in general are discussed. Results of analyses on experimental decays for ethidium intercalated in core particles and in free DNA are reported.

1. Introduction

The fluorescence decay of pure compounds in homogeneous solution is commonly governed by single-exponential decay kinetics, although some compounds may give double- or even triple-exponential decays. Notable examples of biochemical interest are tyrosine (single exponential) and tryptophan (double or triple exponential depending on the solution conditions) [1]. Even when single-exponential pure compounds are introduced as reporter groups into complex systems – proteins, nucleic acids, lipid vesicles, colloidal systems, etc. – they too often show complex decay kinetics, and resolution of double or triple exponentials is common.

In general, the observed complexity may be readily explained in terms of multiple binding sites and multiple rotomeric forms which, because of differences in the local environment, have different decay properties. However, the potential complexity which may arise from such considerations is much greater than even a three-component resolution would indicate. Such arguments lead one to consider the possibility of a distribution of decay times, and the question naturally arises as to whether information on the shape of such distributions may be obtained from the experimental decay data. James and Ware [2] recently described a method of recovering such distributions by using least-squares iterative reconvolution (LSIR) and an exponential series probe function with fixed lifetimes and variable preexponential coefficients. The method has since been applied to the decay of parinaric acid in phospholipid membranes [3]. Livesey and Brochon [4] have described a procedure which may be applicable to time-domain data using a promising new approach called the maximum entropy method; however, the analysis results presented were carried out only on multiex-

Correspondence address: E.W. Small, Department of Biochemistry and Biophysics, Oregon State University, Corvallis, OR 97331-6503, U.S.A.

ponential decay data and no results on decays simulated from distributions were reported. For frequency-domain data, Lakowicz et al. [5] and Alcala et al. [6] independently developed an approach in which a shape for the distribution is assumed (e.g., Gaussian or Lorentzian) and the relevant parameters (centroid, width) are determined by fitting the phase fluorometry data. Lakowicz et al. [5] present several examples of physical phenomena which appear to introduce distributions into fluorescence decays (e.g., spectral relaxation and collisional quenching); they also examined several single-tryptophan proteins and found wide variation in the distribution analysis results. The method as described by Alcala et al. [6] has been used to study a membrane probe in a model system [7] and has been applied to investigation of the effects of temperature and guanidine-induced unfolding on tryptophanyl fluorescence decay from apomyoglobin [8]. These authors have further developed a theory to predict the complex distribution shapes which might be expected for a probe in a macromolecule [9] and have applied the resulting theory using their distribution analysis method to tryptophanyl emission from proteins [10].

The work described here first examines under what circumstances basic information on distributions of lifetimes may be obtainable from time-domain decay data and the degree to which this information may be trusted. We then describe an approach, called the variable filter analysis (VFA) method, which is distinctly different from those described previously, to obtain information on the shape of a presumed distribution. The VFA method does not require any assumptions about the shape of the distribution. The results described here secondly examine the ability of VFA using the method of moments analysis procedure to provide approximations to the shape of simulated distributions and to distinguish true multicomponent decays from decays arising from distributions of lifetimes.

2. Materials and methods

Kiton red, rhodamine 575 and rhodamine 610 were purchased from Exciton (Dayton, OH).

2.1. Instrumentation

The single-photon-counting decay instrument used was as described in ref. 11 except that: (1) an R1564U triple-microchannel-plate photomultiplier was used (Hamamatsu, Middlesex, NJ); (2) the pumping laser was a mode-locked neodymium : YAG laser (Spectra-Physics, Mountain View, CA); and (3) the dye used in the cavity-dumped dye laser was rhodamine 575 in ethylene glycol [12]. Experimental decays were collected at a dye laser pulse rate of 800 kHz and a data collection rate of about 20 kHz using an energy windowing procedure to minimize contributions from pulse pile-up (multiphoton events).

2.2. Simulation of fluorescence decay curves

Simulated decays were generated by numerical convolution of an experimental instrument response function, $E(t)$, with various impulse response functions, $f(t)$. The latter were restricted to sums of exponentials:

$$f(t) = \begin{cases} \sum_{i=1}^{n} \alpha_i \exp[-t/\tau_i] & t \le 0 \\ 0 & t < 0. \end{cases} \quad (1)$$

Where indicated, synthetic multinomial noise was added after scaling the decay to the desired number of total counts.

For our purposes we define a distribution of lifetimes as any $f(t)$ for which adequate data to resolve correctly the constituent decays is unlikely (or impossible) to be obtained experimentally. This definition would include, for example, two very closely spaced decays or a random combination of six or more decays. When a simulation representing a continuous distribution of decays was needed, the distribution function (e.g., a Gaussian, $\alpha(\tau) = \exp[-(\tau - \tau_0)^2/2\sigma^2]$) was sampled at equally spaced τ intervals to give at least 10 decay components in $f(t)$ covering the range over which the $\alpha(\tau)$ was significant. Tests indicated that doubling the number of sampling points would have no significant effect on the results reported here.

The α-weighted average lifetime (A) and the r.m.s. deviation (D) for a sum of exponentials are

computed using standard formulas:

$$A = \sum_1^N [\alpha_i \tau_i] / \sum_1^N \alpha_i$$
$$D^2 = \sum_1^N \left[\alpha_i (\tau_i - A)^2\right] / \sum_1^N \alpha_i. \quad (2)$$

The subscript d (A_d and D_d) will be used to indicate parameters calculated from the α and τ values used to simulate a distribution of lifetimes, the subscript a (A_a and D_a) being used to designate those obtained from a multiexponential analysis of the decay.

In describing results of an analysis on experimental data, or on a simulated decay to which random noise has been added, without showing the actual decay, it is useful to have some measure of the signal-to-noise level in the data. This is commonly done by specifying either the total counts in the decay or the counts in the peak channel. We will include both numbers in the form TC;PC = total counts;peak counts (e.g., TC;PC = 30×10^6; 40×10^3).

2.3. Multiexponential decay analyses

The term 'multiexponential analysis' will be used to indicate results of a normal analysis in which the decay is assumed to arise from a sum of a small number of exponential terms. We generally perform such analyses using the method of moments [13] which is a transform method that does not involve fitting of the experimental data. Analyses were done using moment-index displacement (MD) [14–16] and λ invariance testing [17,18]. Standard methods have been developed for determining the range of the data to be analyzed (out of the usual total of 1024 channels in the decay) and the range of the depression parameter to be tested. A booklet describing the method, the program, and its use is available on request. The approach has also been summarized in a recent article [19].

For many purposes, we have chosen to present results obtained by LSIR analysis because it provides an easily stated criterion (the reduced χ^2 value) which, in the absence of nonrandom errors, can be used to judge the adequacy of the result. The program used, which follows the usual Marquart nonlinear search method, was obtained from Bruce Hudson's group at the University of Oregon and modified minimally, mainly to adapt it to our version of FORTRAN. The range of channels used in the reconvolution was identical to the standard range used for the method of moments (and includes all channels which contribute significantly to the total); the starting point for calculation of the reduced χ^2 values was normally the peak channel of the decay. In those cases for which results are given, the method of moments and least-squares iterative reconvolution (LSIR) analysis methods gave nearly indistinguishable results. Our experience suggests that this will be true if the data do not contain significant nonrandom errors, as is the case for the data from which results are presented here.

2.4. Distribution analysis method

The distribution analysis method used here will be referred to as the variable filter analysis (VFA) method. For a VFA it is first necessary to estimate a range of lifetimes over which the distribution is to be determined. This requires a normal multiexponential analysis of the data, assuming that the decay law is a sum of a few exponentials (1–5) to determine the number of components (n) and their α and τ values; the range of τ to be used for distribution analysis is then chosen to be wider than that obtained by the multiexponential analysis.

For a typical distribution determination, the relative contribution to the decay of a particular lifetime value within this range is estimated using the filter method of Cheng and Eisenfeld [20]. The moments of the impulse response function,

$$G_k = \sum_{i=1}^{n} \alpha_i \tau_i^k \qquad (k = 1, 2, \ldots), \quad (3)$$

once they have been calculated from the original decay data, are filtered to remove the contribution of a filter lifetime, τ_f:

$$G'_k = G_{k+1} - \tau_f G_k = \sum_{i \neq f} \alpha_i (\tau_i - \tau_f) \tau_i^k$$
$$= \sum_{i \neq f} \alpha'_i \tau_i^k \quad (k = 1, 2, \ldots). \quad (4)$$

The filtered moments may be solved simultaneously for the remaining lifetimes and then for their corresponding α values, including the filter α which corresponds to the filter τ. Of course, for a distribution of decay times, the solution for the remaining lifetimes is only approximate, since we can solve only for a relatively small number of decay times. The filter α is then taken as an estimate of the relative amplitude of that decay time in the distribution. A plot of filter α vs. filter τ then represents the distribution.

The starting value for n is usually three but we generally repeat the distribution analysis procedure using four-component filtered analyses, particularly when the multiexponential analysis procedure suggests three or more components. If the four-component distribution analysis differs significantly from the three-component result, a five-component distribution analysis is performed for verification, but this has rarely been found to be necessary. The present version of the VFA analysis program is restricted to a maximum of six components and our experience indicates it will be unlikely that more than six will ever be needed. For very narrow distributions it is not unusual for the four-component analysis to fail (due to computational problems, such as complex roots for a polynomial). In such a case, we normally begin with a two-component distribution analysis which commonly gives results which are verified by the three-component VFA.

In addition to a range for the filter τ, it is necessary to choose a value for the exponential depression parameter (λ) to be used in the distribution analysis. Ideally, the distribution obtained would be independent of λ, in keeping with the rules used in the multiexponential analysis procedure. However, it would be logistically impractical to determine the shape of the distribution over a wide range of λ values in order to find that λ where the shape was least dependent on the depression parameter. Instead, we determine the λ value to be used by varying λ for one point on the distribution (a multiexponential analysis with one lifetime filtered); that point is usually chosen as a filter τ which is about 15% higher than the largest τ value obtained by the multiexponential analysis. Tests indicate that, for the range of λ giving a relatively constant filter α, the final distribution obtained is also relatively independent of the depression over the same range of λ. Although the different moment displacements (MDs) used generally required different values for λ, they usually gave very similar results for the distribution (exceptions are noted in the results which follow).

3. Results and discussion

This section will be divided into four subsections. The first examines the limitations inherent in efforts to analyze for distributions of lifetimes, irrespective of the method used. The second discusses information which may be obtained on lifetime distributions using normal multiexponential analysis procedures. The third subsection illustrates results of distribution analyses on simulated decays using the method of moments VFA procedure described in section 2.4. The final one reports results of such distribution analyses on experimental decays.

3.1. Limitations in distribution analyses

It is obvious that there will be limitations on one's ability to obtain information on lifetime distributions. For example, given a Gaussian distribution of decay times, there will be a width to the distribution below which it will be indistinguishable from a true single-exponential decay. This limiting width can be expected to depend on the signal-to-noise level of the data.

To begin, we analyzed noiseless decays derived from simulated distributions of lifetimes using the normal multiexponential analysis. As a measure of how well the sums of exponentials represented the distribution functions, we report reduced χ^2 values (χ_0^2) given by LSIR analyses. The χ_0^2 value (the subscript 0 will be used to indicate results on noiseless decays) has some useful properties which are masked when synthetic noise is applied. First, the value of χ_0^2 reflects only nonrandom errors in the data, or an insufficiency of the model being fitted to the decay (e.g., not enough components used in the analysis). Second, the sum $1 + \chi_0^2$ is the value which would be obtained from analysis

of an equivalent data set containing random multinomial noise, except that there will be a small deviation (dependent in magnitude on the signal-to-noise ratio) contributed by the random noise. Third, from the $\chi_0^2(TC_1)$ obtained for a decay containing TC_1 total counts, one may accurately estimate the result which would be obtained with a different number of counts, TC_2:

$$\chi_0^2(TC_2) = \frac{TC_2}{TC_1}\chi_0^2(TC_1). \quad (5)$$

Thus, given an n-component analysis of a noiseless simulation at any TC, one may predict the TC which would permit rejection of the n-component analysis and say that the decay consists of at least $(n+1)$ components. (We will make the assumption that a χ_0^2 of 0.1 (no noise), which would result in a χ^2 (with noise) of about 1.1, would be adequate to reject an analysis. This is possible, of course, only in the absence of significant nonrandom errors.)

Fig. 1 shows the χ_0^2 values which result from one-, two- and three-component analyses of noiseless, simulated-distribution decays. They are plotted against D_d/A_d, a measure of the relative width of the distributions (see eqs. 2). The results were obtained for decays with TC;PC = 30×10^6; ~ 190×10^3 CPC: total number of counts in the peak channel), which is near the limit one might attempt using flashlamp technology. With present laser technology, a reasonable limit might be more on the order of 300×10^6 total counts, requiring more than 4 h of data collection time for the decay alone under near-optimal counting conditions. Based on eq. 5, fig. 1 could be adjusted for this increase by taking the curves shown and shifting them up by one unit on the $\log_{10}(\chi_0^2)$ scale.

With 30×10^6 total counts in the decay, a Gaussian distribution of lifetimes will be indistinguishable from a single-exponential decay if the r.m.s. deviation, D_d, is less than 5% of the average lifetime, A_d. Note that this limit will decrease by only a factor of about two for a 10-fold increase in the total number of counts. Similarly, the two-component analysis is unlikely to be rejected until D_d is about 28% of the A_d; and as few as three

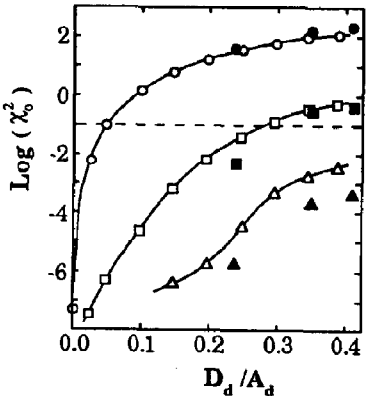

Fig. 1. Effect of distribution width on the LSIR fitting parameter, χ_0^2, obtained for multiexponential analyses of noiseless decays simulated from distributions of decay lifetimes. The parameter D_d/A_d is the ratio of r.m.s. deviation to the average of the corresponding lifetime distribution (calculated according to eq. 2). Results are shown for one- (circles), two- (squares) and three-component (triangles) LSIR analyses of the data. Open symbols represent results obtained for simple Gaussian distributions modeled as 15 exponential decays (14 in the case of $D_d/A_d = 0.4$), symmetric about τ (~ A_d) = 3 ns and equally spaced by 0.4σ (where σ is the standard deviation of the Gaussian, ~ D_d). Filled symbols denote results obtained for more complex distributions. Examples of the lifetime distributions used will be shown in a later figure. The decays were generated by numerical convolution of the sum of exponentials (eq. 1) with an experimental scatter profile. Results are plotted for LSIR analysis of the decays scaled to TC;PC = 30.0×10^6; ~ 190×10^3.

components will be obtained even for very broad distributions ($D_d/A_d > 0.4$). An alternative way of stating these observations is that, at TC;PC = 30×10^6; ~ 190×10^3, a Gaussian distribution of lifetimes will, according to these criteria, be indistinguishable from a two-component decay for $D_d/A_d < 0.2$, etc. From this point of view, it is clear that there are rather severe limitations on one's ultimate ability to distinguish lifetime distributions from multiexponential decays. This conclusion is similar to those drawn by James and Ware [21] and by Lakowicz et al. [5].

3.2. Results using standard analysis procedures

Even if a decay is assumed to arise from a distribution of lifetimes, the normal multiexponential analysis can often reveal important

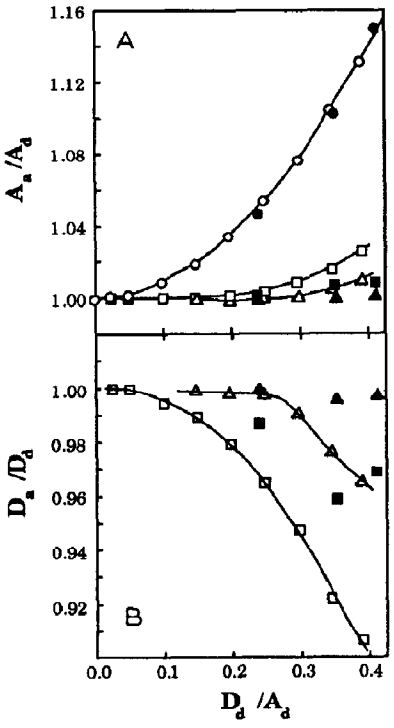

Fig. 2. Comparison of the average lifetime (A_a) and r.m.s. deviation (D_a), calculated from analysis results, to the true distribution average (A_d) and r.m.s. deviation (D_d). The ratios A_a/A_d and D_a/D_d are used as indicators of the deviation from the true values. Symbols: as defined in fig. 1.

basic properties of the distribution. When the decays used for the results in fig. 1 were analyzed as multiexponentials by either method of moments or LSIR, it was noted that, even for reasonably wide distributions (D_d/A_d up to about 0.3), the lifetimes recovered from a two-component analysis corresponded within 10% to $A_d \pm D_d$ (i.e., lifetimes whose average is the α-weighted mean of the distribution and whose separation is twice the r.m.s. deviation).

Further work showed that the α-weighted average lifetimes and r.m.s. deviations, calculated using eqs. 2, were similar whether these parameters were calculated from the distribution used to simulate the decay (A_d, D_d) or from the results of a standard multiexponential analysis (A_a, D_a). Fig. 2 shows plots of A_a/A_d and of D_a/D_d for the distributions used to generate fig. 1. (For the Gaussian distributions, the calculated D_d and A_d values are virtually the same as the defining parameters, σ and τ_0.) The shapes of many of these distributions are shown in fig. 3. The data in fig. 2 were calculated from the LSIR result; however, results using method of moments analysis were very similar. It is apparent (fig. 2A) that even the one-component analysis lifetime ($\tau = A_a$) may provide a reasonably good estimate of A_d (as indicated by $A_a/A_d \sim 1.0$), particularly for the narrower distributions where, as apparent from the discussion of fig. 1, a one-component result may be the only information available. The A_a from two-component results provides an excellent estimate of A_d over the entire range of D_d/A_d with further improvement when the three-component analysis result is used. From fig. 2B it is evident that a reasonable estimate of D_d may also be obtained from the D_a for a two-component analysis result. The three-component D_a gives an even better estimate of D_d. However, the improvement is marginal except for the very broad distributions where it is quite likely that a three-component resolution will be attained (for decays containing 30×10^6 total counts).

3.3. Distribution analysis results on simulated decay data

3.3.1. Results with errorless data

Fig. 3 illustrates results obtained from distribution analyses of a variety of decays. The data used for this figure are 'errorless' in that they contain no intentional nonrandom errors (unintentional errors are introduced during the simulations, however) and no random error (noise). As such, they may be considered equivalent to experimental data collected to an extremely high signal-to-noise level on a nearly perfect instrument (one that introduces little nonrandom error).

The first line of the figure shows results obtained on true one-component and closely spaced two- and three-component decays. Analysis of the single-component decay resulted in a very narrow calculated distribution with a Lorentzian-like shape (note the different abscissa scales used for fig. 3A and D as compared to the other panels). The distribution returned for the two-component

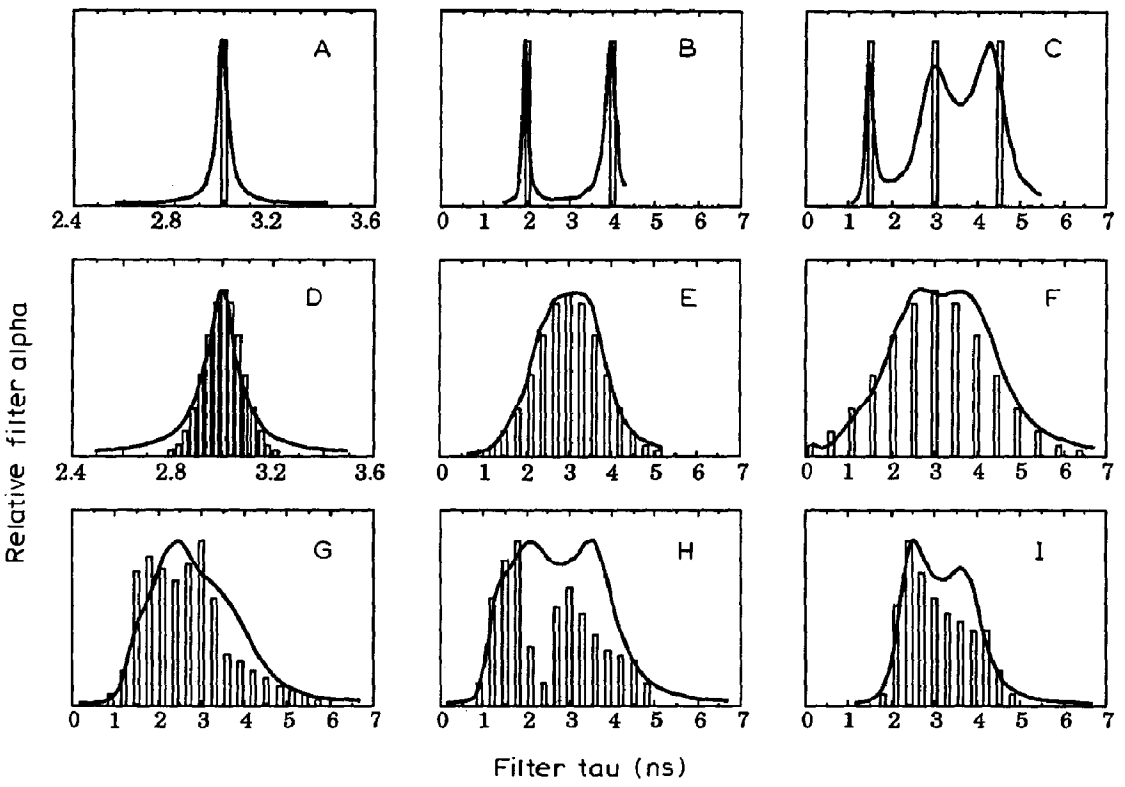

Fig. 3. Examples of distribution analyses obtained for errorless, simulated decay data. Vertical bars represent the α and τ values of the exponential components used to compute the decays. Solid lines denote the results obtained on distribution analysis of the noiseless decays using the VFA method. The actual points defining the curves are not shown for simplicity; they were spaced at 0.1-ns intervals with the exception of panels A, D and B where the spacings were 0.02, 0.02 and 0.033 ns, respectively. Results are shown for decays consisting of: (A) one, (B) two, (C) three components; (D) a narrow Gaussian distribution with $D_d/A_d = 0.025$; (E) a Gaussian distribution with $D_d/A_d = 0.25$; (F) a broad Gaussian distribution yielding $D_d/A_d = 0.39$; (G) a complex distribution giving $D_d/A_d = 0.35$; (H) a complex distribution yielding $D_d/A_d = 0.41$; and (I) a complex distribution giving $D_d/A_d = 0.24$. Distributions D–I are all examples of the data used in generating figs. 1 and 2.

decay (fig. 3B) cleanly resolves the components, but suggests that each consists of a relatively narrow distribution of decay times. For the very closely spaced three-component decay (fig. 3C, which represents a rather difficult resolution problem) the components are not well resolved although there are peaks in the calculated distribution corresponding roughly to the actual lifetimes.

For Gaussian distributions (fig. 3D–F), the calculated results are surprisingly good representations of the shape used to simulate the decays, even for very wide distributions. For the narrow Gaussian ($D_d/A_d = 0.025$) the calculated distribution shows a distinctly Lorentzian shape, with a half-width somewhat less than that of the object distribution and tailing considerably more on both sides. The calculated shape is easily distinguishable from the result for the single-component decay above it. However, it is apparent that it will be essentially impossible to distinguish a Gaussian distribution with $D_d/A_d \leq 0.01$ from a single-component decay, even with 'perfect' data.

The more complex distributions shown in fig. 3G–I represent shapes which have been predicted for fluorescence lifetime distributions in proteins (corresponding to fig. 4a, b and d, respectively, of ref. 8). The shapes of the two narrower distributions (fig. 3G and I) are represented fairly well by

the analysis, although detail has been lost. The result for the broader complex distribution (fig. 3H) is somewhat less representative of the actual shape, giving little evidence of the bimodal nature.

3.3.2. Effects of random noise

Fig. 4 shows distribution analysis results obtained for the data in fig. 3 with random (multinomial) noise added, using 10×10^6 total counts in each decay. The result for the single-exponential decay (fig. 4A) and for the narrow Gaussian (fig. 4D) are both broadened considerably by the noise and have become indistinguishable. The two-component decay (fig. 4B) still shows well-resolved components, although the two peaks have been broadened. The result for the three-component decay suggests two very broad distributions, barely resolved. The level of difficulty which this three-component resolution represents is shown by the result of a multiexponential LSIR analysis (vertical bars in fig. 4) which deviates considerably from the true values.

Where the distribution analysis for the narrow Gaussian was broadened by noise, the result for the middle Gaussian is actually somewhat narrower than was obtained without noise (fig. 3) and tends to tail more on either side of the peak; that for the wide Gaussian was affected little by the

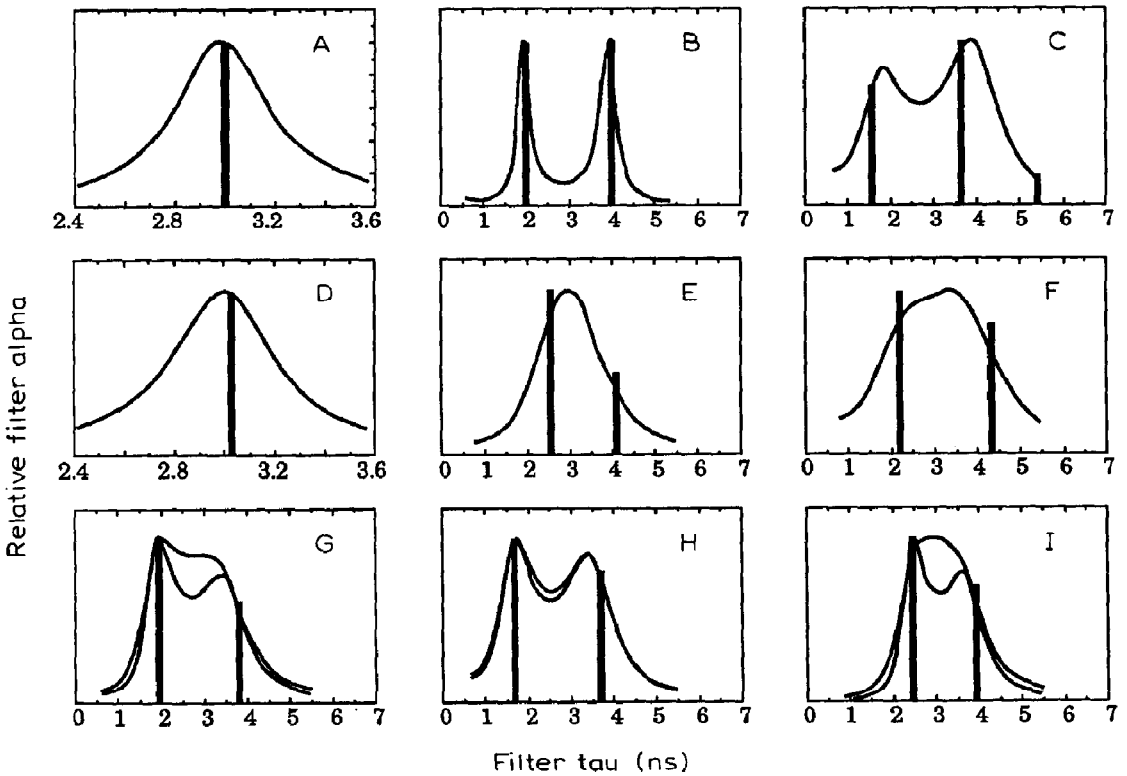

Fig. 4. Effect of random noise on the distribution analysis result. Multinomial noise was added to the data used for fig. 3 after scaling the decays to TC;PC = 10×10^6; ~ 63×10^3 (A–F, I) or 10×10^6; ~ 73×10^3 (G, H). Panels A–I are designated in the same order as that in fig. 3. The solid line shows results obtained by distribution analysis. Two lines are shown when the results using different MD values between 2 and 4 gave differing values; the lines represent two of the resulting curves with the third falling between them. The points defining the curves are not shown for simplicity; they were spaced at 0.1-ns intervals except for panels A and D where the spacings were 0.02 ns. Vertical bars represent results from multiexponential LSIR analyses of the data; the number of components corresponds to the smallest number which gave $\chi^2 \leq 1.1$.

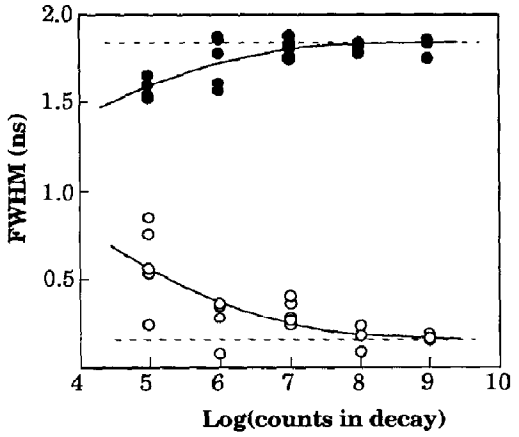

Fig. 5. Effect of random noise on distribution analysis results. Decays were simulated from Gaussian distributions of lifetimes and scaled to a range of total counts. After addition of random (multinomial) noise, the decays were analyzed for distributions of lifetimes. From the resulting curves the full-width-half-maximum (FWHM) values were measured and are plotted as a function of the total counts in the decay. The Gaussian distributions were characterized by D_d/A_d values of 0.025 (equivalent to fig. 3D; ○) and 0.25 (fig. 3E; ●). The FWHM values obtained by analysis of noiseless data are shown as broken lines.

noise. We further characterized the effect of random noise on analysis results for Gaussian distributions of lifetimes. The results are shown in fig. 5 where the effect of noise on the full-width-half-maximum (FWHM) measured from the distribution analysis result is plotted vs. total counts in the decay for data simulated from a narrow (equivalent to fig. 3D) and a wide (fig. 3E) Gaussian distribution of lifetimes. Fig. 5 further shows that the width of the analysis result, as indicated by the FWHM, can vary considerably with different batches of noise, particularly at low signal-to-noise ratios (the shapes were very similar to fig. 4D in all cases). Curiously, while broadening of the result for the narrow Gaussian is greater at smaller number of counts in the decay, the result for the broad Gaussian clearly becomes narrower on average at low total counts. This observation probably reflects a loss of resolution at low counts. At 10×10^6 total counts, the corresponding decay will be indistinguishable from a two-component decay ($D_d/A_d = 0.25$ in fig. 1 after shifting the curves down by 0.5 unit) while at 0.1×10^6 counts the decay will appear to consist of one component (fig. 1, shifted down 2.5 units).

For the complex decays in fig. 4G–I the overall shapes of the analysis results are also affected by the addition of random noise. Curiously, the curves obtained were different for varied values of the moment displacement (MD) used in the analysis, as indicated by the two curves drawn in the figures. In a method of moments multiexponential analysis, disagreement between results at different MDs may indicate that errors in the data are affecting the results. It is interesting that, for the two broader complex distributions, addition of noise has improved the agreement between the analysis result and the shape of the object distribution; this is particularly notable in fig. 4H.

3.3.3. Effects of nonrandom error

There are many types of nonrandom error which may effect decay analysis results [11]. Method of moments analysis using exponential depression and moment index displacement is generally insensitive to such common errors as contamination of the decay with scattered light, time-origin shift and effects of the light frequency on the shape of the measured instrument response. However, nonrandom errors which are not limited to the very short times in the data can affect an analysis [22]. We have investigated the effects on distribution analyses of only one of these, one which could never be completely eliminated even if a perfect decay instrument could be constructed. That error is contamination with background arising from very low level contamination of the sample with (probably multiple) fluorescent species. Fig. 6 shows the results of distribution analyses on the decays used for fig. 3 after addition of a simulated background decay to 0.5% of total counts (no random noise). The effects due to background contamination are surprisingly similar to those obtained for random noise in fig. 4. Calculated distributions for the single exponential and narrow Gaussian are broadened to the point of being indistinguishable; analysis of the contaminated two-component decay gives a distribution which appears as a sum of two rather broad peaks centered near the actual lifetimes used for the

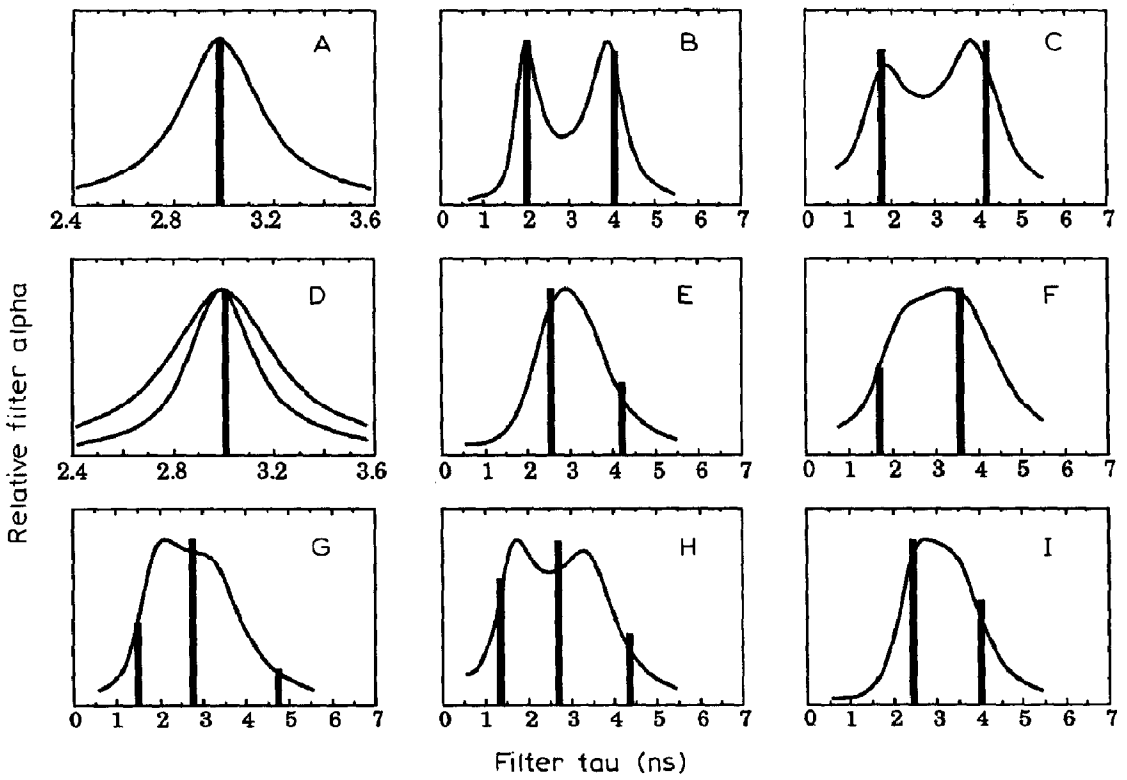

Fig. 6. Effect of nonrandom error (background contamination) on the distribution analysis results. The background decay was simulated from a sum of four components with lifetimes (τ) of 1, 10, 100 and 1000 ns. Preexponential factors were chosen such that $\alpha_i\tau_i$ were the same for all four components. Contaminated decays were generated by adding the background decay to those decays used to generate fig. 3 such that the counts contributed by the background were 0.5% of total counts. The resulting noiseless decays were then analyzed for distributions. A–I correspond to panels A–I in fig. 3. The points defining the curves are not shown for simplicity; they were spaced as for fig. 4. The vertical bars represent results from multiexponential LSIR analyses of the data; the number of components corresponds to the smallest number which gave $\chi^2 \leq 1.1$. In some panels one of the LSIR analysis components is not shown: α,τ = (A) 0.007, 5.6 ns; (D) 0.0007, 42 ns; (F) 0.05, 7.5 ns.

simulation; and the distribution obtained for the three-component decay suggests a badly resolved sum of two distributions. The shapes obtained for the two broad Gaussians are again affected very little by the addition of error. In addition, the results for the complex decays (this time with good MD agreement) are nearly identical to the less structured distributions which are shown in fig. 4.

Fig. 7 shows the effect of various levels of contamination on the FWHM measured from distribution analysis results on decays simulated from a single exponential and from narrow and wide Gaussian distributions of lifetimes. It is evident that very low levels of background contamination (as low as 0.05%) can make it very difficult to distinguish a true single-exponential decay from one arising from a narrow distribution of lifetimes. Also, one observes again that, while increasing contamination increases the width of the distribution obtained for the narrow Gaussian, the width of the result for the broad Gaussian decreases.

3.4. Distribution analysis results on experimental decay data

While there are many experimental systems which may give rise to a distribution of decay times, there are none for which the actual distribu-

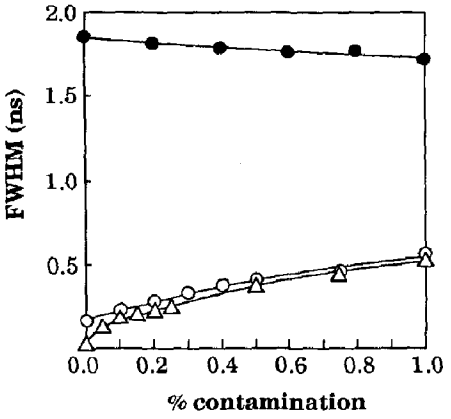

Fig. 7. Effect of different levels of background contamination on distribution analysis results. Decays were simulated from Gaussian distributions of lifetimes and the background in the indicated proportions of total counts. The background decay was the same as that used for fig. 6. The decays, without added random noise, were then analyzed for distributions of lifetimes. From the resulting curves the full-width-half-maximum (FWHM) values were measured and are plotted as a function of the % contamination. The Gaussian distributions were characterized by D_d/A_d values of 0.00 (equivalent to a single exponential, fig. 3A; △), 0.025 (equivalent to fig. 3D; ○), and 0.25 (fig. 3E; ●). The FWHM values obtained by analysis of the errorless data are shown at 0% contamination.

tion is known. This precludes any conclusive test of a distribution analysis method on experimental data. However, it is of interest to see what results may be obtained when experimental decays are analyzed.

To this end, fig. 8 shows results obtained from analysis of experimental decays which showed very good single- and double-exponential characteristics when analyzed by the multiexponential methods. Each of the decays for fig. 8A gave very good single-exponential analyses, with excellent invariance and MD agreement in analysis by the methods of moments and equally good characteristics in the LSIR method (these are among the cleanest single-exponential decays we have encountered). All three examples show narrow distributions, of generally Lorentzian shape, suggesting that the decays arise from single lifetimes or from very narrow distributions of lifetimes as expected for these simple systems. For one case, which gave the best standard analysis result of the three, we estimated the width of the underlying distribution (assumed to be Gaussian) by generating simulations of different widths, with multinomial noise applied at the number of total counts in the experimental decay. Interpolation on the resulting curve of the FWHM of the analysis distribution vs. σ for the input distribution suggested a σ/τ_0 of the order of 0.05. Two-component analyses for the 1.62 and 2.86 ns decays both converged on results suggesting contamination by less than 0.2% of a longer decay with slight improvements in the χ^2 (to 1.02 and 0.90, respectively), suggesting that some broadening due to low-level background may be occurring, as demonstrated in section 3.3. However, for the 3.72 ns decay the two-component analysis converged, with a very small improvement in χ^2 (to 1.057), on a resolution of 3.60 and 3.85 ns with nearly equal amplitudes; this corresponds to $A_a = 3.72$ and $D_a = 0.1227$ which indicate a distribution roughly equivalent to a Gaussian of about $\sigma/\tau_0 = 0.016$. However, one

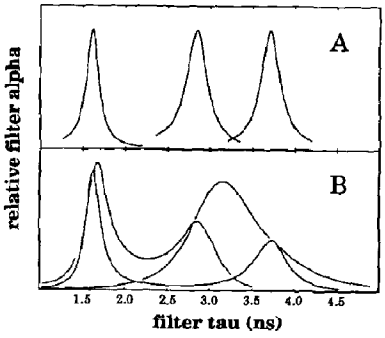

Multiexponential LSIR analysis result

taus	χ^2
1.62	1.13
2.86	0.91
3.72	1.06
1.62, 3.74	1.05
1.65, 2.91	0.93
2.94, 3.92	1.00

Fig. 8. Distribution analysis results for experimental one- and two-component experimental decay data. (A) Results are shown for decays of kiton red in water (1.61 ns, TC;PC = 11.3×10^6;126×10^3), rhodamine 610 in ethanol (2.86 ns, TC;PC = 12.3×10^6;83×10^3), and rhodamine 575 in ethanol (3.72 ns, TC;PC = 11.3×10^6;61×10^3). Excitation was at 289 nm and emission was collected through a Corning CS 3-72 cut-off filter. The points defining the curves are not shown for simplicity; they were spaced at intervals of 0.1 ns. (B) The decays used for panel A were summed in pairs to produce three sets of two-component decay data which were then distribution analyzed to give the results shown. The table to the right lists the decay times and χ^2 values obtained by LSIR multiexponential analysis of the decays; method of moments results were very similar. The spacing between the points which defined the curves was 0.1 or smaller.

must bear in mind that, at the total counts level of 11×10^6, random and nonrandom errors in the data may induce the appearance of background contamination or narrow distribution width.

Fig. 8B shows distribution analysis results on two-component experimental decays formed by summing the single-component decays of fig. 8A (the statistical properties of multinomial noise are preserved as long as the data are summed directly without any scaling). As expected from the results on simulations, when the decay times are widely spaced (1.6 and 3.7 ns) the distribution analysis resolves them quite well, with surprisingly little broadening as compared to the corresponding single-exponential results. The resolution of the 1.6 and 2.9 ns decay components is similar in difficulty level to those shown in figs. 3B, 4B and 6B and the distribution analysis result is very similar to the latter two. Resolution of the 2.9 ns from the 3.7 ns component is too difficult at the signal-to-noise level used and no evidence of bimodal character was obtained, even though in this case multiexponential analyses were able to resolve the decays with relatively little error in the lifetimes (although the preexponential factors showed larger deviations). Distribution analyses on the three-component sum (1.62, 2.86 and 3.72 ns, analysis results not shown) resolved a broadened peak at 1.8 ns from the other two which were again represented by a broader, unresolved peak. In this case, even the standard analyses methods did little better (1.7–1.8 and 3.4–3.5 ns components).

Examples of distribution analysis results on experimental decays from systems which could be expected to result in distributions of lifetimes are shown in fig. 9. The decays were for ethidium bromide intercalated into free DNA and DNA complexed with histone proteins (chromatin core particles). This system can be expected to produce a distribution of decay times, since there may be (at least) 16 distinguishable binding environments depending on which base-pairs are on either side of the intercalated probe. Both method of moments and LSIR multiexponential analyses indicate complex decay kinetics which could be only approximated by sums of exponentials (minimum χ^2 values ranged from 1.2 to 1.7). In fig. 9, panel

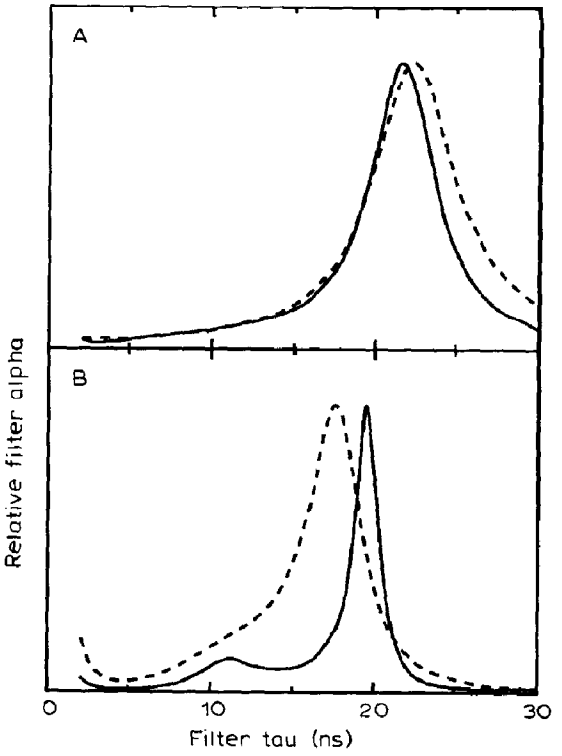

Fig. 9. Distribution analysis results from fluorescence decays of ethidium intercalated in chromatin core particles (solid curves) and in free DNA (dashed curves). Mole ratio of ethidium to DNA base-pairs was either 0.01 (A) or 0.32 (B). Solutions contained 10 mM Tris-HCl, 0.1 mM EDTA, pH 8, and 0.05 mM base-pairs of DNA. Excitation was at 555 nm and emission was collected through a 3 mm Corning CS 2-73 cut-off filter followed by a broad-bandpass interference filter (transmission band of the combination was centered at 593 nm). The TC;PC for the ethidium-DNA data were 30.0×10^6;241×10^3 and 33.4×10^6;385×10^3 for ratios of 0.01 and 0.3, respectively; for the ethidium-core-particle decays the corresponding values were 36.6×10^6;303×10^3 and 34.2×10^6;340×10^3, respectively. The points defining the curves are not shown for simplicity; they were spaced at intervals of 0.5 ns.

A was obtained with an ethidium/base-pair ratio of 0.01 while for panel B the ratio was 0.3. In both cases, the core particles show a narrower distribution than for the DNA, much more so for the higher ratio. At the lower ratio, the average decay time is lower for core particles; this may be due to the resistance of much of the core DNA to initial binding of ethidium (McMurray et al., manuscript

in preparation) which should result in a higher density of binding in those regions which are less resistant. The higher density of bound ethidium results in quenching of the fluorescence, thus decreasing the decay times (as seen for free DNA on going from a ratio of 0.01 to 0.3). The clearly bimodal distributions for both free DNA and core particles at the high ratio are not understood at present, but may indicate a secondary binding mode for the ethidium. (Free ethidium in buffer shows a decay time of 1.6 ns and probably accounts for the upturn in the distribution results at lower decay times.) The core particle DNA appears to be much more resistant than free DNA to very high density binding of ethidium which would account for the lesser quenching at the high ratio.

4. Conclusions

We have presented approaches for obtaining information on distributions of decay times in fluorescence decay analysis without making assumptions about the shape of the distributions. Results of standard multiexponential analyses may be used directly to estimate an average decay time and the r.m.s. deviation of the mean (A_a and D_a, eqs. 2) for the actual distribution. An approach to estimating the shape of the distribution is described which consists of filtering out the contribution of one lifetime while performing an analysis and accepting the preexponential factor resulting for the filter decay time as a measure of its contribution to the distribution. When this is carried out for a range of filter decay times, an approximation for the distribution shape is evolved. Tests of the method on decays simulated from distributions of decay times demonstrate that the method is capable of providing an approximation to the actual distribution shape.

However, one must always bear in mind that, at some level depending on the signal-to-noise ratio in the data to be analyzed, any decay arising from a distribution of decay times will be accurately represented by a sum of exponentials. Nonrandom errors in the data, such as low levels of a contaminant fluorescence which one might expect to encounter routinely, can make it difficult to distinguish between a decay arising from a distribution and one resulting from discrete decay times. Although we have shown this to be true only for the analysis method described here, it is reasonable to expect such effects of random and nonrandom errors on analysis methods in general. Thus, acceptance of a distribution shape, irrespective of the method used to obtain it, or acceptance of discrete decays must imply an implicit assumption of the respective model for the decay law.

Acknowledgments

This work was supported by U.S. Public Health Service grant GM25663. We would like to thank Janet Lee for contributions to many of the computer programs used.

References

1 J.M. Beechem and L. Brand, Annu. Rev. Biochem. 54 (1985) 43.
2 D.R. James and W.R. Ware, Chem. Phys. Lett. 126 (1986) 7.
3 D.R. James, J.R. Turnbull, B.D. Wagner, W.R. Ware and N.O. Petersen, Biochemistry 26 (1987) 6272.
4 A.K. Livesey and J.C. Brochon, Biophys. J. 52 (1987) 693.
5 J.R. Lakowicz, H. Cherek, I. Gryczynski, N. Joshi and M.L. Johnson, Biophys. Chem. 28 (1987) 35.
6 J.R. Alcala, E. Gratton and F.G. Prendergast, Biophys. J. 51 (1987) 587.
7 R. Fiorini, M. Valentino, S. Wang, M. Glaser and E. Gratton, Biochemistry 26 (1987) 3864.
8 E. Bismuto, E. Gratton and G. Irace, Biochemistry 27 (1988) 2132.
9 J.R. Alcala, E. Gratton and F.G. Prendergast, Biophys. J. 51 (1987) 597.
10 J.R. Alcala, E. Gratton and F.G. Prendergast, Biophys. J. 51 (1987) 925.
11 E.W. Small, L.J. Libertini and I. Isenberg, Rev. Sci. Instrum. 55 (1984) 879.
12 L.J. Libertini and E.W. Small, Anal. Biochem. 163 (1987) 500.
13 I. Isenberg and R.D. Dyson, Biophys. J. 9 (1969) 1337.
14 I. Isenberg, J. Chem. Phys. 59 (1973) 5696.
15 E.W. Small and I. Isenberg, Biopolymers 15 (1976) 1093.
16 E.W. Small and I. Isenberg, J. Chem. Phys. 66 (1977) 3347.
17 J.W. Lee, J. Chem. Phys. 77 (1982) 2806.

18 I. Isenberg and E.W. Small, J. Chem. Phys. 77 (1982) 2799.
19 E.W. Small, L.J. Libertini, D.W. Brown and J.R. Small, in: Fluorescence detection II, ed. E.R. Menzel (SPIE Proceedings vol. 1054, 1989) p. 36.
20 S.W. Cheng and J. Eisenfeld, in: Applied nonlinear analysis, ed. V. Lakshmikantham (Academic Press, New York, 1979) p. 485.
21 D.R. James and W.R. Ware, Chem. Phys. Lett. 120 (1985) 455.
22 L.J. Libertini and E.W. Small, Rev. Sci. Instrum. 54 (1983) 1458.